HHS Public Access

Author manuscript

J Mol Cell Cardiol. Author manuscript; available in PMC 2016 October 01.

Published in final edited form as:

J Mol Cell Cardiol. 2015 October ; 87: 4–16. doi:10.1016/j.yjmcc.2015.07.020.

De-novo Collateral Formation Following Acute Myocardial Infarction: Dependence on CCR2^{+} Bone Marrow Cells

Hua Zhang and **James E Faber**

Department of Cell Biology and Physiology and the McAllister Heart Institute, University of North Carolina at Chapel Hill

Abstract

Wide variation exists in the extent (number and diameter) of native pre-existing collaterals in tissues of different strains of mice, with supportive indirect evidence recently appearing for humans. This variation is a major determinant of the wide variation in severity of tissue injury in occlusive vascular disease. Whether such genetic-dependent variation also exists in the heart is unknown because no model exists for study of mouse coronary collaterals. Also owing to methodological limitations, it is not known if ischemia can induce new coronary collaterals to form ("neo-collaterals") versus remodeling of pre-existing ones. The present study sought to develop a model to study coronary collaterals in mice, determine whether neo-collateral formation occurs, and investigate the responsible mechanisms. Four strains with known rank-ordered differences in collateral extent in brain and skeletal muscle were studied: C57BLKS>C57BL/6>A/J>BALB/c. Unexpectedly, these and 5 additional strains lacked native coronary collaterals. However after ligation, neo-collaterals formed rapidly within 1-to-2 days, reaching their maximum extent in ≤ 7 days. Rank-order for neo-collateral formation differed from the above: C57BL/6>BALB/c>C57BLKS>A/J. Collateral network conductance, infarct volume^{-1}, and contractile function followed this same rank-order. Neo-collateral formation and collateral conductance were reduced and infarct volume increased in MCP1$^{-/-}$ and CCR2$^{-/-}$ mice. Bone-marrow transplant rescued collateral formation in CCR2$^{-/-}$ mice. Involvement of fractalkine→CX_3CR1 signaling and endothelial cell proliferation were also identified. This study introduces a model for investigating the coronary collateral circulation in mice, demonstrates that neocollaterals form rapidly after coronary occlusion, and finds that MCP→CCR2-mediated recruitment of myeloid cells is required for this process.

Keywords

collateral circulation; coronary circulation; genetic background; myocardial infarction; hematopoietic cells

Corresponding Author: James E Faber, Department of Cell Biology and Physiology, 111 Mason Farm Rd, University of North Carolina at Chapel Hill, Chapel Hill, NC 27599-7545, 919-966-0327 (office), 919-966-6927 (fax), jefaber@med.unc.edu.

Disclosures

None.

1. Introduction

Most tissues have a native collateral circulation composed of infrequent arteriole-to-arteriole anastomoses that cross-connect the crowns of adjacent arterial trees [1–6]. The pressure drop that occurs across them after a sudden occlusion in the trunk of one of the trees causes blood to flow across the collateral network. By providing an alternative route for flow, collaterals can significantly lessen ischemic injury depending on their number and diameter, ie, "extent". In animal models of sustained arterial obstruction, collaterals in the brain and lower extremities remodel (enlarge) their anatomic lumen diameter by shear stress-induced and, depending on the tissue, hypoxia-induced processes that require days-to-weeks for completion [1–7]. The ability of remodeling to reduce final infarct volume depends on the collateral extent at baseline before obstruction, the volume of ischemic penumbra or border zone surrounding the necrotic core, the tolerance of the tissue to ischemia, how rapid remodeling occurs, and how much collateral diameters increase. Collateral remodeling in heart, where these vessels are difficult to image directly, is believed to underlie the progressive increase with time in collateral-dependent flow in animal models of and patients with acute myocardial infarction (MI), coronary artery disease (CAD) and acute coronary syndrome [1–6].

Indirect measures of collateral-dependent blood flow suggest that native collateral extent in heart, brain and lower extremities varies greatly among "healthy" humans, ie, in the absence of CAD [4] or peripheral artery disease [8] or when assessed in the hyper-acute phase of ischemic stroke [9,10], ie, conditions where remodeling—which can also vary among individuals [1–7,11–15]—has not yet taken place. This variation at baseline has been suggested to be a major determinant of the wide variation in the severity of tissue injury when arterial obstruction develops [4,5,7,9–15]. Consistent with these studies, among patients in which thrombolytic treatment failed to elicit reperfusion during the acute phase of MI, those with "good/high" collateralization had 35% smaller infarct volumes [16]. Similarly, in patients with CAD, those with good collaterals had a 36% lower mortality risk than those with poor collaterals [4]. The cause of this variation in collateral circulation is unknown. However, recent studies in mice have found that differences in genetic background may be a major factor [5,7,12–15]. Collateral extent in brain varied 46-fold among 21 strains of mice [14], with large variation also present in skeletal muscle and intestine examined in several of the same strains [11–13]. The differences correlated with wide differences in tissue injury in models of acute and chronic arterial obstruction in brain (eg, 30-fold variation in infarct volume [7]) and lower extremities [12,13]. Approximately 85 percent of the variation in both collateral extent and tissue injury was recently linked to a polymorphic genetic locus (*Dce1*), which when introgressed from a strain with abundant collaterals into one with poor collaterals, completely rescued the collateral deficit and functional outcome attributable to the locus [15]. This locus is thus a critical link in the pathway that directs collaterogenesis, ie, formation of native collaterals. In mouse brain [17,18] and human heart [19] collaterogenesis occurs during development after the general arterial-venous circulation has formed, and in mouse determines collateral extent in the adult.

Whether such genetic variation in native collaterals also exists in heart to explain the above findings in humans [4,16] is unknown because of absence of methods to study the coronary collateral circulation in mice—the mammalian species most amenable to genetic manipulation. This presumably is because of the complex three-dimensional arrangement of the coronary circulation and difficulty in distinguishing collaterals from other vessels (problems not confined to mice), phasic contraction of the heart which in mouse exceeds 550 beats per minute, small size of the mouse heart, and difficulty in studying its coronary circulation. It is also not known if occlusive disease can induce new coronary collaterals to form. It has generally been assumed [1] (but not without exception [3]) that only remodeling of native collaterals occurs after arterial stenosis or occlusion. However, this assumption remains uncertain because of limitations in resolution of previous angiographic methods: native collaterals can be as small as the smallest arterioles in a tissue (~6–8 microns diameter), are thousands-fold less abundant than nearby arterioles (eg, in skeletal muscle [11]), and can only be anatomically differentiated from the latter by identifying their anastomotic connections. Once collaterals have remodeled after arterial occlusion, their many-fold larger diameter and increased tortuosity makes them somewhat easier to identify. However, the number then detected would reflect native collaterals that have remodeled and —if in fact it occurs—*de novo* formation of additional ones ("neo-collaterals"[5]). And neither native collaterals nor neo-collaterals could be distinguished from each other based on diameter, since the amount of remodeling of native collaterals would depend on their baseline diameter [7,13] (the primary determinant of shear stress) and the vigor of the pathways controlling the remodeling process [1–6], while the final diameter of any neo-collaterals that formed would reflect the process of *de novo* collateral formation.

To address the above questions, we first optimized methods to study the coronary collateral circulation in mice, namely high resolution three-dimensional angiography, measurement of conductance of the collateral network, and histology on single identified collaterals. An unexpected finding followed: mice lack a native collateral circulation in heart even though they have collaterals in their other tissues. This surprising outcome, however, allowed us to unambiguously ask whether new collaterals form after arterial obstruction. Patent neo-collaterals indeed appeared rapidly within 1-to-2 days after acute MI and achieved their maximal number and diameter within 7 days. Neo-collateral formation varied with genetic background. Strains with greater formation had greater collateral conductance, smaller final infarct volumes, and better recovery of contractile function. However, the strain-specific pattern differed from that seen for differences in extent of the native collateral circulation in brain and other tissues of the same strains [7,12,13], indicating that different mechanisms direct collaterogenesis in the embryo and neo-collateral formation in the ischemic adult heart. In addition, we found that bone-marrow-derived myeloid cells and MCP1→CCR2, and to a lesser degree fractalkine→ CX_3CR1 signaling, were required. This study provides a model to study new collateral formation after acute myocardial infarction that may identify novel targets for treatment of ischemic disease.

2. Methods

See the online Data Supplement for additional details.

2.1. Animals

Mice, guinea pigs and rats were male and 3–5 months-old, except in the following experiments: inbred strains of mice on day-1 after ligation; measurement of retrograde fill time and infarct volume; bone marrow transplants; CCR2 and CX_3CR1 marker mice. These used ~equal numbers of male and female mice.

2.2. Coronary ligation, micro-angiography, morphometry, collateral conductance

The left anterior descending coronary artery was ligated 3mm below the left atrial margin (LADX) to produce a small infarction of 10–20% of left ventricle-plus-septum (LVS) wall volume, thus minimizing stimuli for compensatory hypertrophy and vascular growth that otherwise occurs in the normal (remote) myocardium following a large MI [3]. Approximately 99% survival occurred. Proximal ligation to produce a larger infarction (~45% of LV volume) was also examined in a separate group of B6 mice, wherein ~50% survived without evidence of heart failure as reported previously [20]. Immediately or specified days after LADX, mice received one or more of the following after administration of heparin, maximal dilation with papavarine and nitroprusside, and fixation with paraformaldehyde to prevent any subsequent constriction ("hep-dil-fix"): 1) arterial angiography following infusion of Microfil^{R} and optical clearing to determine the number and lumen diameter of neo-collaterals within the border zone connecting distal branches of the LAD to adjacent circumflex, right coronary and septal arterial trees; 2) measurement of either the time^{-1} required to backfill the LAD tree to the point of ligation with Microfil or microsphere trapping (both administered at a constant inflow pressure) to determine the relative "conductance" or blood flow, respectively, of the nascent collateral network; 3) perfusion of Evans blue-in-phosphate buffered saline (PBS) to determine the territory of the LAD tree below the ligation.

2.3. Infarct volume, dp/dt analysis, histology, cell proliferation, apoptosis, bone marrow

transplantation Infarct volume was measured using 2,3,5-triphenytetrazolium chloride staining (TTC) and cardiac function using dp/dt analysis. Histology was performed for neo-collaterals that were identified after hep-dil-fix, filling and clearing by: 1) their cross-connecting the LAD and adjacent arterial trees, and 2) retension of Microfil in their lumen following dissection of the tissue micro-block containing the collateral and sectioning at 8-microns. To determine cell proliferation, EdU (5-ethynyl-2′-deoxyuridine) was injected on day-2 and day-4 after LADX, followed by dissection of neo-collateral-containing tissue blocks on day-7. Bone marrow transplant was performed to generate EGFP;B6-transgenic mice and 4 reciprocol CCR2$^{-/-}$;C57BL/6 (B6) chimeras.

2.4. Statistical analysis

Data (mean±SE) underwent *t*-tests, ANOVA, Bonferroni tests, or linear regression ($p<0.05$ = significant). Where possible, data were collected by investigator blinded to treatment group.

3. Results

3.1. Mice lack native coronary collaterals

We used an angiographic casting method previously used to quantify native collaterals in other tissues of mouse [7,11–15]. Surprisingly, no coronary collaterals were present in B6 mice (Figure 1) or 7 other inbred strains [C57BLKS (BLKS), A/J, BALB/cBy (BALB/c), C3H-He, CBA, DBA/2, SJL (n≥5 each)], nor in CD1 outbred mice (n=3). This was unexpected since these strains have native collaterals in brain and other tissues where they are: most abundant in BLKS, abundant in B6, CBA, DBA/2, SJL, CD1, C3H-He, less abundant in A/J, and least abundant in BALB/c [7,13,15]. Absence of coronary collaterals was irrespective of sex.

To confirm this unexpected finding that, unlike other mammals extending from rat to human [4,21–23], mice lack native coronary collaterals, we used 5 additional methods to be certain that coronary collaterals with very small diameters had not escaped detection: 1) casting with low-viscosity Microfil or with high pressure to insure filling of the capillary bed (Figure 1C, Online Figures 1,2); 2) casting after minimizing resistance downstream of any extant native collaterals by transection of the LAD just distal to its point of ligation (Figure 1D,E); 3) perfusion with Evans blue-PBS (viscosity same as water; Online Figures/Videos 3–5); 4) endothelial staining with either intravascular IB4-lectin-Alexa-568, or 5) using endothelial ephrin-B2$^{LacZ/+}$ transgenic mice on both B6 and BALB/c backgrounds (data not shown). No collaterals were detected with any of these additional methods. Only capillaries (Figure 2) were present within the watershed zone between adjacent arterial trees. They averaged 4.7 microns in diameter, thus our methods can readily detect the smallest vessels in the mouse heart.

We wondered if the absence of coronary collaterals in the mouse species is due to the steep increase in heart rate that occurs during the first several weeks after birth (350 on postnatal day- 0–1 rising to 550–650 beats per minute in the young adult) [24,25]. We reasoned that the phasic blood flow and pressures unique to the coronary circulation might create—in mouse with its short diastolic intervals—hemodynamic conditions in nascent collaterals favoring their regression. That is, it is known that chronic level of shear stress influences growth of the native coronary collateral circulation: conductance of the coronary network correlates directly with the time in diastole, which is when the majority of coronary perfusion occurs [3,29,30]; after birth the proportion of time in diastole declines since heart rate rapidly increases to 550–600 bpm as mice grow to sexual maturity [24]. Despite this reasoning, collaterals were also absent in in VECAD$^{GFP/+}$ pups on postnatal day-1 and-2 (data not shown) and in 3 week-old B6 mice (Online Figure 6), when formation of native collaterals in other tissues has achieved the number and diameter present in the adult [17,18].

To further validate our casting method, we confirmed as a positive control its ability to detect collaterals in guinea pigs and rats. These species have been shown, either by measuring infarct volume or collateral-dependent flow (microspheres) shortly after ligation [21,22], or using angiography in rat [23], to have abundant and sparse native coronary collaterals, respectively. Guinea pigs do not sustain infarctions after proximal LADX,

leading to the assumption that they have abundant collaterals [21,22]. The data in Online Figure 7 show this assumption is correct. Collectively, the above findings using 5 different methods plus positive "controls" demonstrate that, unlike other mammalian species examined by ourselves and others [21–23], mice lack native collaterals in heart despite having them in their other tissues.

3.2. *De novo* formation of collaterals occurs rapidly after coronary occlusion

It has long been assumed that only remodeling of native collaterals occurs after arterial occlusion. Our findings that mice lack native coronary collaterals provided an opportunity to address this question directly, since unlike in previous studies, no pre-existing collaterals exist to complicate interpretation of results *vis-à-vis* collateral remodeling.

An exciting result occurred after distal LADX. New collaterals ("neo-collaterals"[5]) began forming within 1-to-2 days and reached their maximum number and diameter within 4-to-7 days, ie, ~10 collaterals cross-connecting to distal branches of the LAD with an average lumen diameter of ~18 μm; no significant change in number or diameter was observed after 7 days (Figure 2, Online Figure 8). Placing the suture knot adjacent to the LAD (sham LADX) had no effect. Ligation 2mm proximal to the standard ligation used above and elsewhere in this study, which caused a larger infarction (~45% of left ventricular volume) where once again no native collaterals were detected, caused twice as many neo-collaterals to form by day-7 (Online Figure 9).

3.3. Variation in neo-collateral formation, collateral network resistance, and severity of infarct volume accompany differences in genetic background

Previous studies in mice found that native collateral number and diameter (collateral extent) in brain, skeletal muscle and intestine vary widely with genetic background [7,13 –15]. This variation closely correlated with a similarly wide variation in the same strains in severity of tissue injury following arterial occlusion. Linkage, SNP-association among 21 strains, and congenic analyses showed that a single locus, *Dce1*, is responsible for 85% of this variation [14,15]. Strain-specific differences in native extent in the adult are specified during formation of the collateral circulation (collaterogenesis), which occurs during the perinatal period [17,18]. To determine if ischemic neo-collateral formation in adult heart also varies with genetic background in a manner suggesting linkage to *Dce1*, we performed LADX on 4 strains with the largest rank-order difference in native collateral extent (in brain and other tissues) among 21 strains [14]: BLKS > B6 > A/J > BALB/c. If variants of the *Dce1* allele also mediate variation in neo-collateral formation in ischemic heart, the latter should follow this same rank-order. However, BALB/c mice formed neo-collaterals with a similar number, diameter and 14-day time-course as shown in Figure 2 for B6 mice, although number was lower on day-14 in BALB/c ($p<0.05$, data not shown); moreover, BLKS and A/J strains formed fewer collaterals of smaller diameter (Figure 3A,B). Thus the rank-order for neo-collateral formation in heart does not follow the rank-order for native collaterogenesis in other tissues of these strains, suggesting different underlying mechanisms.

To examine the functional significance of neo-collateral formation, we developed a method to estimate relative resistance/conductance of the collateral network supplying the territory

below the ligation, based on transit time for retrograde filling of low-viscosity Microfil^{R} back to the point of ligation of the LAD ("retrograde fill-time"; Figure 3C, Online Figure/Video 10). As expected from the data in Figure 2E, no filling occurred at day-0 and day-1 after ligation in B6 mice (Figure 3C's inset bar graph); fill-time then declined ~exponentially. Also as expected from Figure 3A,B, fill-time one week after LADX, when maximal neo-collateral formation was achieved, varied inversely with strain-dependent variation in formation (Figure 3C). Unlike the above data for neo-collateral formation which were for male mice, fill-time was determined using both male and female BALB/c and B6 mice (n=6–7 of each sex). No sex-specific difference was seen (p=0.60). We also measured infarct volume 1 week after LADX in both sexes. As predicted from the relative resistances in Figure 3C, the rank-order for infarct volume followed the rank-order for retrograde fill-time (Figure 3D), resulting in a close correlation (Figure 3E) that did not differ with sex. Because we used a small-infarction model to avoid heart failure and the accompanying myocardial cell disturbances, we were unsuccessful in detecting significant deficiency in pump function on day-7 using echocardiography (Vivo 2100, Visualsonics Inc). However, contractile function as assessed by dP/dt analysis demonstrated that A/J mice exhibited greater deficits than B6 (Figure 4A). These findings are not due to differences in territory of the LAD tree below the ligation (Online Figure 11).

Baseline data: Body weight for 3–5 months-old male B6, BALB/c, BLKS and A/J strains did not differ, and none of the above data correlated with body weight, arterial pressure or heart rate for the strains (see Online Methods for data). Although cardiac function assessed in these strains at baseline by the same lab has not been reported, some data are available. B6 and BALB/c body:heart weight ratio did not differ [20,26], whereas dP/dt+ was greater in B6 but dP/dt−, LVEDP, LVESP and tau did not differ [26]. In isolated hearts, these metrics did not differ between B6 and BALB/c (and 6 other strains not including BLKS and A/J) at baseline, after 20 minutes of ischemia, and after 60 minutes of reperfusion (differences were seen, however, using in vivo, albeit open-chest, PV loop analysis) [27]. Cardiac function assessed by echocardiography and radiotelemetry did not differ between B6 and BALB/c [20,28].

The above results demonstrate that neo-collateral formation varies with genetic background, is independent of sex, and results in closely correlated variation in ischemic tissue damage and deficits in developed pressures; these data do not associate with differences in baseline parameters.

3.4. Nascent neo-collaterals and surrounding bone marrow-derived cells types

To begin to understand the mechanisms underlying neo-collateral formation in ischemic heart, we performed histology on single neo-collaterals identified after filling, optical clearing, microdissection of the tissue block surrounding the collateral, and sectioning—wherein microfil was retained in the collateral lumen of the tissue sections as an additional confirmation (see Online Figure 12 for methods). Seven days after LADX, monocytic and myocardial cells were evident in the vicinity of the neo-collaterals in the border zone/shoulder region (Figure 4B,C). Neo-collaterals were invested with αSMA^{+} cells having the morphology of smooth muscle cells (Figure 4E). Interestingly, cardiomyocytes were

commonly seen adjacent to venules and collaterals in the infarcted region next to the border zone (Figure 4B,C). This has been reported previously for venules [29,30].

We transplanted bone marrow from B6;GFP constitutive ubiquitously expressing transgenic mice into wildtype B6 mice. Seven days after LADX, lectin$^+$/GFP$^+$ bone-marrow derived cells (BMC) were present in the border zone and vicinity of nascent collaterals (Online Figure 13; see also Figure 7A–D). Less abundant lectin$^-$/GFP$^+$ (Online Figure 13, white stars) and lectin$^+$/GFP$^-$ cells (red stars) were also present. It is possible that the former are bone marrow-derived CX_3CR1^+ macrophages (confirmed below). Similar results were obtained using direct fluorescence instead of anti-GFP immunohistochemistry (Online Figure 13). CD45$^+$/lectin$^+$ and CD45$^+$/lectin$^-$ cells were also present (Online Figure 13E,F). In contrast, both cell types were less abundant in MCP1$^{-/-}$ and CCR2$^{-/-}$ mice (Online Figure 13G,H). Perivascular CD34$^+$/lectin$^-$ cells were also evident (Online Figure 14). No GFP$^+$ BMCs or CD45$^+$ or CD34$^+$ cells were observed in the neo-collateral wall, thus no evidence for engraftment of hematopoietic cells (Figure 5, Online Figures 13,14). Retrograde fill-time was not altered in mice genetically deficient for lymphoid cells (38±5 versus 37±6 seconds; n=6 each of nude mice and their wildtype (het) controls (Nu/J, #002019, outbred population, Jackson Labs)). This indicates that T-cells are not required for neo-collateral formation.

3.5. Neo-collateral formation is dependent on MCP1→CCR2 signaling

Given the above finding of several myeloid cell types adjacent to nascent collaterals, we tested the hypothesis that monocyte chemoattractant protein-1 (MCP1) is required for ischemic collaterogenesis. MCP1 is released from cardiomyocytes, ECs, SMCs, and a variety of hematopoietic and other cell types in ischemic, injured, inflamed and tumorigenic tissues and binds CCR2 receptors that are present on monocytes, CD4 T-cells, ECs, endothelial progenitor cells (EPCs) and mesenchymal stem/stromal cells (MSCs) [31–33]. MCP1→CCR2 signaling is a major effector of homing of BMCs, adhesion to endothelium, transmigration, and secretion of additional MCP1 and other chemokines and cytokines. Neo-collateral formation was reduced and infarct volume increased in MCP1$^{-/-}$ and CCR2$^{-/-}$ B6 mice (Figure 5). The smaller effect of deletion of MCP1 compared to CCR2 on neo-collateral formation and absence of effect on retrograde fill-time may reflect contribution and/or compensation by other MCP family members that also bind CCR2 [31–34]. Microsphere trapping was used to confirm the ability of the fill-time method (Figure 3) to estimate collateral-dependent flow, and to confirm its reduction in CCR2$^{-/-}$ mice as predicted by the above results (Online Figures 15,16). Given the possible presence of CX_3CR1^+ M2 macrophages in the vicinity of developing neo-collaterals (Figure 5A–D, Online Figure 13, see also below), we examined $CX_3CR1^{-/-}$ B6 mice. Neo-collateral diameter but not number was reduced (Figure 5).

These results indicate that MCP→CCR2 and to a lesser extent fractalkine→CX_3CR1^+ signaling pathways are required for neo-collateral formation. Consistent with this, CD45$^+$/lectin$^+$ and CD45$^+$/lectin$^-$ cells were less abundant in the vicinity of the smaller (and fewer) neo-collaterals that formed in MCP1$^{-/-}$ and CCR2$^{-/-}$ mice (Online Figure 13G,H). Likewise, 5 days after ligation of CCR2$^{RFP/+}$ and $CX_3CR1^{GFP/+}$ reporter mice (B6

background, Jackson Labs), CCR2- and CX_3CR1-expressing cells were strongly recruited to the border zone and found in close proximity to neo-collaterals (Figure 6). Both cells types were also present in much fewer numbers 1 day after LADX (data not shown). Potential EPCs/hematopoietic precursors were also evident as $Flk1^+$ cells not expressing $CCR2^{RFP/+}$ or $CX_3CR1^{GFP/+}$. αSMA^+ staining identified abundant myofibroblast-like cells in the interstitium and presence of mural cells displaying the morphology of pericytes and SMCs (Figure 6B–E, Figure 5E).

To confirm the above conclusion that $CCR2^+$ cells have a major role in ischemic collaterogenesis, to test whether they are recruited from bone marrow versus elsewhere, and to address the fact that $CCR2^{-/-}$ mice have reduced monocyte egress [34], we did bone marrow transplants of B6 and $CCR2^{-/-}$;B6 mice (Figure 7). Transplant of wildtype BMCs into $CCR2^{-/-}$ mice rescued neo-collateral formation by 73% (Figure 7E). In addition, transplant of $CCR2^{-/-}$ BMCs to wildtype mice inhibited neo-collateral formation by the same amount as in $CCR2^{-/-}$ mice. Autologous reconstitution of wildtype and knockout mice BMCs showed no effect of the transplant procedure *per se* (Figure 7E). Of note, the small infarct model we employed produced endocardial infarctions in the territory at risk (Figure 7A,C), with diffusion of oxygen from the ventricular lumen and epicardial arteries presumably protecting the subendocardium and epicardium, respectively. Consistent with this, we found neo-collaterals only formed within the endocardium where hypoxia and pressure gradients across the capillary plexus in the watersheds would be the greatest (discussed below).

Compared to B6 mice, neo-collaterals of A/J and $CCR2^{-/-}$ showed reduced EC proliferation at day-7 (Online Figure 18), consistent with the fewer collaterals of smaller diameter that these strains form. Collateral endothelial cells that had undergone proliferation over the 7 days of pulse-labeling were widely dispersed. This pattern is inconsistent with the notion that neo-collateral formation begins with formation of new capillaries cross-connecting adjacent trees to the LAD (see Discussion). No apoptosis was observed within the walls of neo-collaterals, although occasional apoptotic cells were seen in the vicinity (Online Figure 19).

4. Discussion

A surprising finding in this study is that mouse heart lacks native coronary collaterals, given that the strains we examined have collaterals in their brain, skeletal muscle, intestine and skin (ear) [7,11–15,35]. Absence of coronary collaterals, as assessed immediately after ligation, was not due to failure to detect them. We used the same filling and optical clearing methods that we have used to determine collateral number and diameter in other tissues, including in strains of mice with collaterals that are both few in number and small in diameter (ie, BALB/c and A/J) [7,13–15]. Also, as positive controls we confirmed reports suggesting that rat has sparse [21,23] and guinea pig abundant [21,22] collaterals. We employed five additional methods that filled or stained capillaries, ie, the smallest vessels in heart that averaged 4.7 microns in diameter: use of Microfil at lower-viscosities or higher pressures than used above; reducing downstream resistance by transection of the LAD below the ligation before infusion of Microfil; endothelial staining with LacZ in ephrin-

$B2^{LacZ/+}$ mice or with lectin (staining was followed by optical clearing); perfusion with saline containing Evans blue dye. None of these methods detected native collaterals. All of the above methods were conducted after maximal dilation and fixation at this maximum. This absence was not a function of genetic background. No collaterals were found in nine strains that span the range, among 21 inbred and wild-derived strains, from most-to-least number of collaterals in their non-heart tissues (eg, ~30 in the neocortex of BLKS versus 0-to-1 in BALB/c) [7,13–15,17].

The apparent absence of coronary collaterals in mouse is unique among mammals studied. Injection of microspheres after acute ligation of the circumflex artery identified a native coronary collateral circulation in all eight non-murine mammalian species examined [21]. However, collateral flow as indicated by percent of microspheres trapped in the ischemic versus non-ischemic (remote) zone varied widely. Collateral flow was 100% in guinea pig, 16% in dog, 12% in cat, 6% in rat, and “low” in 4 species, ie, 2% in ferret, baboon and rabbit, and 1% in pig. The accuracy of these values may have been affected by not administering heparin and a smooth muscle dilator followed by a fixative (as used herein), use of 15 micron microspheres whose presence in the ischemic zone will vary with collateral diameter, and possible presence within the dissected ischemic zone of microsphere-containing distal-most arterioles from the surrounding non-ischemic trees. However, infarct volumes measured at 1.5, 3 and 6 hours after acute ligation for several of the species are qualitatively consistent with these differences (guinea pig = no infarction, cat > dog > rabbit = pig) [22]. Nevertheless, it is noteworthy that only a single inbred strain of each species was examined (ie, Dunkin-Hartley guinea pig, greyhound dog, Wistar rat, New Zealand White rabbit) [21] or likely-to-be closely interbred/related individuals (ie, ferret, baboon) or breed-stock (pig, breed not given) [21.22]. Given the wide variation in native collateral extent among different mouse strains [7,13–15] and collateral-dependent flow among “outbred” humans [4,8–10], the often-stated conclusion that these findings [21] are due to species-specific variation in native collaterals requires confirmation using either wild or genetically diverse individuals from each species. In fact, while references cited therein [21] are consistent for guinea pig (however some reports found mild ischemia after ligation, plus there are few commercial strains available), other references therein report that collateral flow ranges from 10–30% in dog, is greater in cat than dog, is less than 0.01% in rat, ranges from low-to-15% in baboon, and that there is disagreement in rabbit and pig (breeds were not given). Elsewhere, Dalland landrace pigs had abundant native collaterals on bismuth filling (but 15 micron microspheres yielded a collateral flow of 0.06%—a disagreement that the authors suggested could reflect edema-induced vascular compression) [36]. In contrast, a recently developed high-resolution three-dimensional imaging technique detected few native coronary collaterals in Yorkshire pigs [37]. Notwithstanding methodological limitations, the above reports are consistent with the concept that native collateral extent varies among species and among different strains and breed-stock within a species. However, our finding that mice lack native collaterals apparently regardless of strain (we did not study wild mice and ~500 other inbred strains) is unique among species examined.

We can only speculate on why the above-mentioned larger mammals have native coronary collaterals while mouse does not. One possibility, predicated on a second speculation [5], is that collaterals in healthy tissues, by contributing flow from an adjacent tree to a locally

metabolically dilated region of a given tree, help to optimize or fine-tune regional oxygen delivery to meet regional oxygen demand, particularly in tissues that exhibit large changes in metabolic rate and high oxygen demand (eg, striated muscle, brain). This optimization would include within the watershed region/zone between adjacent arterial trees, where terminal arterioles can be seen branching from collaterals [7]. Given the small size of the mouse heart, its watersheds may be sufficiently narrow (eg, Figures 1,6) that diffusion of oxygen is adequate and collaterals are not needed to “scaffold” terminal arterioles. While this may explain why mouse heart lacks native collaterals, it does not explain why there is a strain difference in neo-collateral formation for the same size infarction and area at risk. We presume the latter is due to gene variants among the strains in the cells and signaling pathway that drive neo-collateral formation (discussed below). The hypothesis that native collaterals may, in the absence of obstruction, serve to optimize oxygen supply-to-demand, and thus that hypoxia-related adaptive mechanisms may exist to increase collateral extent is supported by the finding that chronic anemia in dogs, pigs and humans is accompanied by increased collateral conductance [38.39 and references therein]. However, anemia caused biventricular hypertrophy and growth of the overall coronary circulation. Thus, the extent to which the effect of anemia reflects remodeling of pre-existing collaterals, caused by a pressure difference across them [1,6,22] as well as local hypoxia [2,3], and/or neo-collateral formation remains to be determined.

The most important finding of our study is that patent collaterals formed after coronary ligation. A long-standing controversy has existed regarding whether collateral-dependent perfusion, which begins to increase in hindlimb by three days after arterial obstruction and continues to increase for several weeks afterwards [1–6,11–13,15], is due only to outward remodeling of native collaterals (arteriogenesis) or also depends on formation of additional collaterals (neo-collaterals). This uncertainty extends in part from the difficulty in distinguishing pre-existing collaterals from much more abundant nearby arterioles. It has generally been assumed that only remodeling of native collaterals occurs. Our finding that mice lack pre-existing coronary collaterals provided an opportunity to address this controversy since no native collaterals exist to complicate interpretation of results *vis-à-vis* collateral remodeling. This is the first study to show that new collaterals form physiologically in the ischemic heart. That this can be induced to occur surgically comes from the observation that trans-positioning a length of the intact mammary artery and attendant perivascular tissue and vasa vasorum onto the ischemic region of the myocardium of patients with CAD resulted in more than 50% of the implants establishing connectivity to the arterial circulation within the territory at risk [40]. And an anatomically analogous surgical procedure is used to treat certain types of cerebral arterial occlusions [41]. Neo-collateral formation following arterial occlusion has been reported in brain [7] and skeletal muscle [42] of strains of adult mice that have low numbers of native collaterals. Although the mechanism was not examined, neo-collateral formation was not seen in strains with abundant collaterals, leading us to hypothesize that this was because the ischemic region in these strains was well-removed from the watersheds where collaterals form, ie, that *de-novo* collateral formation requires ischemia (discussed below). An important future question is whether neo-collateral formation occurs in species, including human, endowed with native

coronary collaterals. The above studies in mouse brain and skeletal muscle support the possibility.

Collaterals and retrograde perfusion of the—interestingly, still-intact and patent LAD tree—appeared rapidly by day-2. This is similar to brain, where patent neo-collaterals were not seen at day-1.5 after arterial ligation but were present by day-3 [7], and in skeletal muscle where they were not evident at day-2 but present by day-4 [42]. Collateral formation is faster than the onset of growth of arterioles in the surviving (remote) myocardium, which was seen 7 days after a large MI in association with increased wall stress and compensatory hypertrophy [3]. Nevertheless, coronary neo-collateral formation is too slow to prevent development of a necrotic core, which occurs within ~30 minutes after ligation [3,4,43,44]. Importantly however, blood-borne immune cells delivered to the core via collaterals, as opposed to the otherwise much slower route via migration through the vascular wall and interstitium, would be expected to speed removal of cell debre, reduce the amount and duration of inflammation, and aid delivery of circulating mesenchymal fibroblast precursors. This would favor more efficient scar formation, oppose adverse ventricular remodeling, and improve recovery of pump function. Interestingly, scar volume related inversely to the number of visible collaterals in patients [44]. Of equal or more importance, neo-collateral formation would also be expected to reduce the volume and severity of ischemia and accompanying injury in hibernating myocardial cells in the outermost territory of the occluded tree and its adjacent watersheds/border zones. This would promote salvage of a portion of the area at risk, leading to a smaller final infarct volume. Neo-collateral formation would also speed delivery of cardiac and vascular progenitor cells to this area, which evidence suggests promote myocardial repair, neo-vascularization, favorable chamber remodeling, and recovery of function [1–4,45–55]. Although additional studies will be required to examine these hypotheses, our findings that infarct volume and heart function closely associate with the extent of neo-collateral formation in mice with differences in genetic background and mice genetically deficient in MCP1 or CCR2 are consistent with a beneficial effect of collateral formation even if it does not begin until 1-to-2 days after acute myocardial infarction. Interestingly, Zhang et al found in pigs that intracoronary injection of labeled $CD34^+$ BMCs upstream of LAD ligation done two weeks earlier increased Rentrop-score, pump function, vessel density, SDF-1 and bFGF, and $CD34^+$ cells in the vicinity of vessels in the peri-infarct region when examined several weeks later [56]. Furthermore, these effects were more pronounced in pigs that had greater Rentrop scores at the time of injection, leading the authors to suggest that collaterals serve as a conduit to aid homing of BMCs to ischemic myocardium leading to better recovery of function.

Mice genetically deficient in T-cells evidenced no deficit in neo-collateral formation, thus myeloid but not lymphoid cells are required. Formation required MCP1 and CCR2 receptor signaling, since it was inhibited by ~50% in $MCP1^{-/-}$ and $CCR2^{-/-}$ mice. This conclusion was confirmed with deficiency and rescue experiments using CCR2 bone marrow chimeras and histological identification of bone-marrow derived $CCR2^+$ cells in the vicinity of nascent neo-collaterals using genetic reporter mice. Hypoxia/ischemia, increased fluid shear stress, and myocardial and SMC cell stretch, which are all present in the border zone, induce expression of VEGF from cardiomyocytes and ECs which in turn express MCP1 [1–4,6,22,54,55]. MCP1 increases within hours after acute MI in infarct and border zones and is

sustained through day-28 in mouse [57,58]. In humans, serum levels are not elevated early-on but rise from 12–24 weeks [58]. MCP1stimulates release, homing to heart, EC adhesion, and diapedesis of $CCR2^+$ BMCs and monocytes which are skewed by CCR2 activation to the M1 macrophage ($CCR2^+$, CX_3CR1^{low}, $lectin^-$, $CD45^+$) —IL6/1β, TNFα-expressing inflammatory phenotype that itself also releases MCP1 [59,60]. Monocytes, T-cells, EPCs, SMCs and mesenchymal stem/stromal cells (MSCs) are $CCR2^+$ [31–33]. Consistent with a role for M1 monocytes and progenitor cells in neo-collateral formation, we detected fewer $lectin^-/CD45^+$, $lectin^-/CD34^+$ cells around nascent neo-collaterals in $MCP1^{-/-}$ and $CCR2^{-/-}$ mice that both formed fewer collaterals in association with lower collateral network conductance and greater infarct volumes. We also found less EC proliferation in neo-collaterals of $CCR2^{-/-}$ and A/J mice, in agreement with their deficit in neo-collateral number, diameter and network conductance. Interestingly, MCP1 is protective in post-MI ischemia-reperfusion, and MCP1→CCR2 activity decreases adverse ventricular remodeling [49,61–63]. However, MCP1 may also be harmful, a paradox that may relate to fibrosis and remodeling [61,63]. Recently, Arslan and coworkers [48] found that patients with CAD and abundant coronary collaterals on Rentrop had increased numbers of peripheral monocytes and the $CD14^{++}/CD16^-$ subset (also known as $CCR2^+/CX_3CR1^{low}$ M1 classical monocyte/macrophage). Morimoto et al [49] demonstrated that mice with cardiac overexpression of MCP1 had reduced infarct volume and adverse chamber remodeling two weeks after coronary ligation. However, whether these results reflect neo-collateral formation and/or remodeling cannot be determined, since it is well-known that MCP1→CCR2 signaling also contributes to collateral remodeling in animals [1,3,6,22,55] and is associated with increased Rentrop grade after MI in patients [46,47,54]. Of note, we found that neo-collateral formation was inhibited less in $MCP1^{-/-}$ than $CCR2^{-/-}$ mice. MCP1–4, CCL12 and CCL16 ligate CCR2 [31], and MCP3 can mediate homing of MSCs to the ischemic heart [64] and induce coronary smooth muscle cell proliferation in vitro [65]. Thus more than one CCR2 ligand may be involved in neo-collateral formation or compensate in the absence of MCP1.

Macrophages are polarized in vitro toward M2 phenotypes by IL-4 and IL-13 (M2a), immune complex-FcγR/TLR (M2b), and IL-10,TGF-β and glucocorticoids (M2c) [59,60]. Ischemic/inflammatory myocardium and ECs and SMCs release fractalkine (CX_3CL1) to recruit $CCR2^{lo}$-CX_3CR1^{hi} M2 monocytes to the ischemic area via CX_3CR1 [6]. Macrophage and SMC cross-talk via fractalkine→CX_3CR1 signaling enhances expression of TNFα, IL-1β, IL-6, CX_3CR1 and matrix metalloproteinases [66]. Fractalkine has anti-apoptotic and proliferative effects on SMCs [67–70]. Secretion of these proteins and their cross-talk promote differentiation of $\alpha SMC\text{-}actin^+$ mural cells. Fractalkine, the only member of the CX_3C chemokine family, is membrane-bound through the chemokine domain which attaches via a mucin-like stalk to the cell surface. It is expressed on neurons, epithelial cells, macrophages, and at low levels on ECs, SMCs and cardiomyocytes, while CX_3CR1 is expressed by monocytes, natural killer cells, T-cells and SMCs [67–70]. Its expression is increased in heart by infarction, heart failure and inflammation [67–70]. In the present study, involvement of fractalkine→CX_3CR1 signaling in neo-collateral formation was indicated by its partial inhibition in $CX_3CR1^{-/-}$ mice and by histological evidence using genetic reporter mice for CX_3CR1^+ cells in the vicinity of nascent neo-collaterals. Other cell types and

signaling pathways are likely involved in the complex process of neo-collateral formation [1–4,6,32,33,45,54,55,58,71–78].

Figure 7F presents a model for neo-collateral formation. The capillary plexus within watershed zones is interconnected and receives blood flow from the surrounding arterial trees that normally returns via the contiguous venous trees down the path of least resistance [3,79]. We confirmed these findings in mice (Online Figures 3–5). We propose that arterial obstruction causes, within the watersheds, ischemia and increased fluid shear stress toward the territory at risk, especially in the largest-diameter capillaries. The latter are relatively few in number in capillary plexi in adult heart [3]. Induced expression of MCP1, fractalkine and other factors activate CCR2, CX_3CR1 and other proteins, leading to recruitment of myeloid and vascular progenitors and other cell types from bone marrow and possibly intra- and other extra-cardiac tissue sites. Factors from heart and vascular cells and extracellular matrix are also released locally. The resulting milieu of growth and remodeling factors includes ones that direct pruning over day-0-to-1 of venous connections from these activated large capillaries, followed by EC proliferation and an increase in the capillary's diameter and length and recruitment of mural cells over day-1-to-7. The concept of pruning of capillary side-branches that would otherwise divert flow to the contiguous venous trees draining the adjacent non-ischemic regions is supported by findings of Le Noble et al (and in other studies referenced therein) [80]. Arterial obstruction caused unfavorable angles of shear stress at the side-branches of certain capillaries within the chick yolk-sac plexus. This was accompanied within hours by migration of ECs to close off the side-branches, followed by growth of the capillaries into large-diameter collateral-like anastomoses within 24 hours. Reorganization of ECs and modest proliferation but not apoptosis were seen; we also confirmed the latter two for neo-collateral formation.

Our model does not include a requirement for sprouting capillary angiogenesis, given the rapid time-course for onset of neo-collateral formation and retrograde perfusion (Figures 2 and 3). Also, the pattern of proliferation of collateral ECs (Online Figure 18) during the 7 days of pulse-labeling after LADX, ie, widely separated ECs rather than large numbers of adjacent ECs, does not fit the pattern expected for newly formed capillaries. Proliferation of ECs and additional muralization by SMCs after day-7 would further increase diameter and length of the nascent collaterals, resulting in the characteristic tortuous morphology seen by day-14 and thereafter (Figure 2). We did not detect involvement of apoptosis (albeit staining was confined to day-7), or evidence of proliferation of αSMC^+ cells by EdU labeling. We thus propose that muralization arises from differentiation of pericytes or fibroblasts or their mesenchymal precursors into SMCs. SMCs could also migrate from the distal-most arterioles anastomosed by the nascent collateral. We found little evidence for engraftment of CCR2- or CX_3CR1-positive cells (Figure 6) or other bone-marrow derived cells (Online Figures 13,14), and it was not possible to determine if occasional positive cells close-to/within the collateral wall were undergoing diapedesis (Figure 6B,C). In contrast, marker-expressing cells in the vicinity of the neo-collaterals were much more abundant (Figure 6, Online Figures 13,14), supporting a paracrine role for these cells. Interestingly, injection of pericytes into the border zone following acute MI in mice supported myocardial repair [81].

The above model differs significantly from how native collaterals form during the perinatal period (collaterogenesis), a process that determines the extent of the native collateral circulation in the adult [17,18]. Collaterogenesis does not appear to require ischemia or increased shear stress. Instead, it consists of an angiogenic-like arteriolar sprouting mechanism that begins in the last third of gestation and that is followed by SMC muralization requiring several weeks to reach completion [18]. Collaterogenesis has thus far been shown to involve the *Dce1* locus [15] and NFκB→VEGF-A→Flk1→synectin→notch→Dll4→ADAM-10,-17 signaling, as well as Cnx-37,-40 and CLIC4 [18 and references therein,82,83]. The present study shows that neo-collateral formation in the ischemic heart varies with genetic background, but with a strain-specific pattern different from that seen for the differences in collaterogenesis that occur in the same strains. This indicates that different mechanisms direct collaterogenesis and neo-collateral formation. The basis for the difference in collateral formation among these strains is not known. Of note, the pattern for thioglycolate-induced accumulation of macrophages into the peritoneum was B6>BALB/c>A/J and for MCP1 levels in peritoneal fluid was B6<BALB/c=A/J [84], consistent with the role of MCP1→CCR2 signaling in neo-collateral formation.

Neo-collateral formation also differs from collateral remodeling. Remodeling requires, among other BMCs, T cells [1,6,54,55] that were not required for neo-collateral formation. Remodeling also requires increased shear stress but not ischemia in the vicinity of the collaterals in hindlimb models [1.22]. In contrast, ischemia is present in the watershed/borderzone region of the heart after acute MI [2,3,7], where native collaterals reside and neo-collaterals form. Yet both mechanisms require recruitment of paracrine-acting myeloid cells and MCP1→CCR2 and fractalkine→CX_3CR1 signaling [1,6,54,55]. Interestingly, native collateral extent in brain and hindlimb is not altered in $MCP1^{-/-}$ mice (Online Figure 20). This is consistent with our evidence discussed above, as well as the requirement for MCP1 signaling for collateral remodeling in hindlimb as shown by others [1,6,22], that the signaling pathway that stimulates neo-collateral formation differs from that directing collaterogenesis and collateral remodeling in tissues studied thus far.

In conclusion, this is the first study to examine whether new collaterals can form in the adult heart. We were aided by the unexpected finding that mice lack a native coronary collateral circulation, as this permitted us to eliminate remodeling of pre-existing collaterals after acute MI as a confounder. Although this absence is unique among mammals studied, there is evidence that a significant percentage of humans have poor coronary collaterals [4]. Neo-collateral formation was rapid and accompanied by smaller infarcts and better recovery of heart function. Bone-marrow-derived myeloid cells and MCP1→CCR2 and fractalkine→CX_3CR1 signaling were required, with little evidence for engraftment. We also found that neo-collateral formation varied with genetic background, and with a pattern suggesting the underlying pathway differs from that responsible for formation of the native collateral circulation during development. By reducing ischemia and speeding delivery of immune and progenitor cells, neo-collaterals may promote rescue of ischemic cardiomyocytes and regeneration of new ones thus lessening infarct progression, promote efficient scar formation, protect against unfavorable remodeling, and thus improve recovery

after acute MI. This study presents a model and set of methods to investigate these questions. Previous trials of therapies shown in animal studies to augment angiogenesis and collateral remodeling have met with limited success [1–4,54,55,85]. While many factors have been suggested to underlie this discordance, an understanding of the biology of neo-collateral formation may lead to identification of novel genes/pathways to test in patients, including those where surgical revascularization is not an option, to enhance recovery.

Supplementary Material

Refer to Web version on PubMed Central for supplementary material.

Acknowledgements

The authors are grateful to Kirk McNaughton and Ashley Ezzell for histological sectioning and cyano-Massons staining, and to Robert Currin and the UNC-Olympus Imaging Research Center.

Sources of Funding

NIH-NHLBI HL111070 (JEF).

Non-standard Abbreviations and Acronyms

αSMA	α-smooth muscle actin
B6	C57BL/6 mouse strain
BLKS	C57BLKS mouse strain
BMC	bone marrow-derived cell
CAD	atherosclerotic coronary artery disease
CCR2	chemokine CC motif receptor-2
CX_3, CR1	chemokine CXC motif receptor-1
CCL	chemokine CC motif ligand
EdU	5-ethynyl-2´-deoxyuridine
EC	endothelial cell
EPC	endothelial progenitor cell
LADX	left anterior descending coronary artery ligation
dp/dt+/−	derivative of left ventricular pressure rise/fall
LVED/SP	left ventricular end-diastolic/systolic pressure
MI	myocardial infarction
MCP1	monocyte chemoattractant protein-1
MSC	mesenchymal stem/stromal cell
SDF1	stromal-derived factor-1
SMC	smooth muscle cell

TTC	2,3,5-triphenyltetrazolium chloride
WT	wildtype

References

1. van Royen N, Piek JJ, Schaper W, Fulton WF. A critical review of clinical arteriogenesis research. J Am Coll Cardiol. 2009; 55:17–25. [PubMed: 20117358]
2. Chilian WM, Penn MS, Pung YF, Dong F, Mayorga M, Ohanyan V, Logan S, Yin L. Coronary collateral growth--back to the future. J Mol Cell Cardiol. 2012; 52:905–911. [PubMed: 22210280]
3. Tomanek, JR. Coronary Vasculature: Development, Structure-Function, and Adaptations. Springer US Inc; 2013.
4. Seiler C, Stoller M, Pitt B, Meier P. The human coronary collateral circulation: development and clinical importance. Eur Heart J. 2013; 34:2674–2682. [PubMed: 23739241]
5. Faber, JE.; Dai, X.; Lucitti, J. Genetic and environmental mechanisms controlling formation and maintenance of the native collateral circulation. In: Deindl, E.; Schaper, W., editors. Arteriogenesis – Molecular Regulation, Pathophysiology and Therapeutics I. Vol. 1. Aachen, GE: Shaker Verlag; 2011. p. 1-22.
6. Meisner JK, Price RJ. Spatial and temporal coordination of bone marrow-derived cell activity during arteriogenesis: regulation of the endogenous response and therapeutic implications. Microcirculation. 2010; 17:583–599. [PubMed: 21044213]
7. Zhang H, Prabhakar P, Sealock R, Faber JE. Wide genetic variation in the native pial collateral circulation is a major determinant of variation in severity of stroke. J Cereb Blood Flow Metab. 2010; 30:923–934. [PubMed: 20125182]
8. Traupe T, Ortmann J, Stoller M, Baumgartner I, de Marchi SF, Seiler C. Direct quantitative assessment of the peripheral artery collateral circulation in patients undergoing angiography. Circulation. 2013; 128:737–744. [PubMed: 23817577]
9. Shuaib A, Butcher K, Mohammad AA, Saqqur M, Liebeskind DS. Collateral blood vessels in acute ischaemic stroke: a potential therapeutic target. Lancet Neurol. 2011; 10:909–921. [PubMed: 21939900]
10. Al-Ali F, Elias JJ, Filipkowski DE, Faber JE. Acute ischemic stroke treatment, part 1: Patient Selection. “The 50% barrier and the capillary index score. Front Neurol. 2015; 6:83. [PubMed: 25954243]
11. Moore SM, Zhang H, Maeda N, Doerschuk, Faber JE. Cardiovascular risk factors cause premature rarefaction of the collateral circulation and greater ischemic tissue injury. Angiogenesis. 2015; 18:265–281. [PubMed: 25862671]
12. Chalothorn D, Clayton JA, Zhang H, Pomp D, Faber JE. Collateral density, remodeling and VEGF-A expression differ widely between mouse strains. Physiol Genomics. 2007; 30:179–191. [PubMed: 17426116]
13. Chalothorn D, Faber JE. Strain-dependent variation in native collateral function in mouse hindlimb. Physiol Genomics. 2010; 42:469–479. [PubMed: 20551146]
14. Wang S, Zhang H, Wiltshire T, Sealock R, Faber JE. Genetic dissection of the *Canq1* locus governing variation in extent of the collateral circulation. PLoS One. 2012; 7:e31910. [PubMed: 22412848]
15. Sealock R, Zhang, Lucitti JL, Moore SM, Faber JE. Congenic fine-mapping identifies a major causal locus for variation in the native collateral circulation and ischemic injury in brain and lower extremity. Circ Res. 2014; 114:660–671. [PubMed: 24300334]
16. Habib GB, Heibig J, Forman SA, Brown BG, Roberts R, Terrin ML, Bolli R. Influence of coronary collateral vessels on myocardial infarct size in humans. Results of phase I thrombolysis in myocardial infarction (TIMI) trial. The TIMI Investigators. Circulation. 1991; 83:739–746. [PubMed: 1900223]
17. Chalothorn D, Faber JE. Formation and maturation or the murine native cerebral collateral circulation. J Molec Cell Cardiol. 2010; 49:251–259. [PubMed: 20346953]

18. Lucitti JL, Mackey J, Morrison J, Haigh J, Adams R, Faber JE. Formation of the collateral circulation is regulated by vascular endothelial growth factor-A and A Disintegrin and Metalloprotease Family Members 10 and 17. Circ Res. 2012; 111:1539–1550. [PubMed: 22965144]
19. Reiner L, Molnar J, Jimenez FA, Freudenthal RR. Interarterial coronary anastomoses in neonates. Arch Pathol. 1961; 71:103–112. [PubMed: 13740594]
20. van den Borne SW, van de Schans VA, Strzelecka AE, Vervoort-Peters HT, Lijnen PM, Cleutjens JP, Smits JF, Daemen MJ, Janssen BJ, Blankesteijn WM. Mouse strain determines the outcome of wound healing after myocardial infarction. Cardiovasc Res. 2009; 84:273–282. [PubMed: 19542177]
21. Maxwell MP, Hearse DJ, Yellon DM. Species variation in the coronary collateral circulation during regional myocardial ischaemia: A critical determinant of the rate of evolution and extent of myocardial infarction. Cardiovasc Res. 1987; 21:737–746. [PubMed: 3440266]
22. Schaper, W.; Piek, JJ.; Munoz-Chapuli; Wolf, C.; Ito, W. Collateral circulation of the heart. In: Ware, JA.; Simons, M., editors. Angiogenesis and Cardiovascular Disease. Oxford Univ Press; 1999. p. 163
23. Toyota E, Warltier DC, Brock T, Ritman E, Kolz C, O'Malley P, Rocic P, Focardi M, Chilian WM. Vascular endothelial growth factor is required for coronary collateral growth in the rat. Circulation. 2005; 112:2108–2113. [PubMed: 16203926]
24. Zehendner CM, Luhmann HJ, Yang JW. A simple and novel method to monitor breathing and heart rate in awake and urethane-anesthetized newborn rodents. PLoS One. 2013; 8:e62628. [PubMed: 23658756]
25. Smolock EM, Ilyushkina IA, Ghazalpour A, Gerloff J, Murashev AN, Lusis AJ, Korshunov VA. Genetic locus on mouse chromosome 7 controls elevated heart rate. Physiol Genomics. 2012; 44:689–698. [PubMed: 22589454]
26. Lerman I, Harrison BC, Freeman K, Hewett TE, Allen DL, Robbins J, Leinwand LA. Genetic variability in forced and voluntary endurance exercise performance in seven inbred mouse strains. J Appl Physiol. 2002; 92:2245–2255. [PubMed: 12015333]
27. Barnabei MS, Palpant NJ, Metzger JM. Influence of genetic background on ex vivo and in vivo cardiac function in several commonly used inbred mouse strains. Physiol Genomics. 2010; 42A: 103–113. [PubMed: 20627938]
28. Shah AP, Siedlecka U, Gandhi A, Navaratnarajah M, Al-Saud SA, Yacoub MH, Terracciano CM. Genetic background affects function and intracellular calcium regulation of mouse hearts. Cardiovasc Res. 2010; 87:683–693. [PubMed: 20413651]
29. Christensen LP, Zhang RL, Zheng W, Campanelli JJ, Dedkov EI, Weiss RM, Tomanek RJ. Postmyocardial infarction remodeling and coronary reserve: effects of ivabradine and beta blockade therapy. Am J Physiol Heart Circ Physiol. 2009; 297:H322–H330. [PubMed: 19411283]
30. Zhang RL, Christensen LP, Tomanek RJ. Chronic heart rate reduction facilitates cardiomyocyte survival after myocardial infarction. Anat Rec (Hoboken). 2010; 293:839–848. [PubMed: 20225200]
31. Deshmane SL, Kremlev S, Amini S, Sawaya BE. Monocyte chemoattractant protein-1 (MCP-1): An overview. J Interferon Cytokine Res. 2009; 29:313–326. [PubMed: 19441883]
32. Walenta KL, Bettink S, Bohm M, Friedrich EB. Differential chemokine receptor expression regulates functional specialization of endothelial progenitor cell subpopulations. Basic Res Cardiol. 2011; 106:299–305. [PubMed: 21174211]
33. Belema-Bedada F, Uchida S, Martire A, Kostin S, Braun T. Efficient homing of multipotent adult mesenchymal stem cells depends on frount-mediated clustering of CCR2. Cell Stem Cell. 2008; 2:566–575. [PubMed: 18522849]
34. Tsou CL, Peters W, Si Y, Slaymaker S, Aslanian AM, Weisberg SP, Mack M, Charo IF. Critical roles for CCR2 and MCP-3 in monocyte mobilization from bone marrow and recruitment to inflammatory sites. J Clin Invest. 2007; 117:902–909. [PubMed: 17364026]
35. Cheng G, Zhang H, Yang X, Tzima E, Ewalt KL, Schimmel P, Faber JE. Mini-tyrosyl-tRNA synthetase regulates ischemic angiogenesis, leukocyte recruitment, and vascular permeability. Am J Physiol. 2008; 295:R1138–R1146.

36. de Groot D, Grundmann S, Timmers L, Pasterkamp G, Hoefer IE. Assessment of collateral artery function and growth in a pig model of stepwise coronary occlusion. Am J Physiol Heart Circ Physiol. 2011; 300:H408–H414. [PubMed: 20952668]

37. van den Wijngaard JP, Schulten H, van Horssen P, Ter Wee RD, Siebes M, Post MJ, Spaan JA. Porcine coronary collateral formation in the absence of a pressure gradient remote of the ischemic border zone. Am J Physiol Heart Circ Physiol. 2011; 300:H1930–H1937. [PubMed: 21398599]

38. Eckstein RW. Development of interarterial coronary anastomoses by chronic anemia; disappearance following correction of anemia. Circ Res. 1955; 3:306–310. [PubMed: 14364770]

39. Scheel KW, Williams SE. Hypertrophy and coronary and collateral vascularity in dogs with severe chronic anemia. Am J Physiol. 1985; 249:H1031–H1037. [PubMed: 2932919]

40. Vineberg A, Munro DD, Cohen H, Buller W. Four years' clinical experience with internal mammary artery implantation in the treatment of human coronary artery insufficiency including additional experimental studies. J Thorac Surg. 1955; 29:1–32. [PubMed: 13222472]

41. Gonzalez NR, Liebeskind DS, Dusick JR, Mayor F, Saver J. Intracranial arterial stenoses: current viewpoints, novel approaches, and surgical perspectives. Neurosurg Rev. 2013; 36:175–184. [PubMed: 23097149]

42. Mac Gabhann F, Peirce SM. Collateral capillary arterialization following arteriolar ligation in murine skeletal muscle. Microcirculation. 2010; 17:333–347. [PubMed: 20618691]

43. Dedkov EI, Zheng W, Tomanek RJ. Compensatory growth of coronary arterioles in postinfarcted heart: regional differences in DNA synthesis and growth factor/receptor expression patterns. Am J Physiol Heart Circ Physiol. 2006; 291:H1686–H1693. [PubMed: 16714360]

44. Bexell D, Setser RM, Schoenhagen P, Lieber ML, Brener SJ, Ivanc TB, Balazs EM, O'Donnell TP, Stillman AE, Arheden H, Wagner GS, White RD. Influence of coronary artery stenosis severity and coronary collateralization on extent of chronic myocardial scar: insights from quantitative coronary angiography and delayed-enhancement MRI. Open Cardiovasc Med J. 2008; 2:79–86. [PubMed: 19337359]

45. Deindl E, Zaruba MM, Brunner S, Huber B, Mehl U, Assmann G, Hoefer IE, Mueller-Hoecker J, Franz WM. G-CSF administration after myocardial infarction in mice attenuates late ischemic cardiomyopathy by enhanced arteriogenesis. FASEB J. 2006; 20:956–958. [PubMed: 16571777]

46. Park HJ, Chang K, Park CS, Jang SW, Ihm SH, Kim PJ, Baek SH, Seung KB, Choi KB. Coronary collaterals: The role of MCP-1 during the early phase of acute myocardial infarction. Int J Cardiol. 2008; 130:409–413. [PubMed: 18158188]

47. Sahinarslan A, Kocaman SA, Topal S, Ercin U, Bukan N, Yalcin R, Timurkaynak T. Relation between serum monocyte chemoattractant protein-1 and coronary collateral development. Coron Artery Dis. 2010; 21:455–459. [PubMed: 20859200]

48. Arslan U, Kocaoglu I, Falay MY, Balc M, Duyuler S, Korkmaz A. The association between different monocyte subsets and coronary collateral development. Coron Artery Dis. 2012; 23:16–21. [PubMed: 22045058]

49. Morimoto H, Takahashi M, Izawa A, Ise H, Hongo M, Kolattukudy PE, Ikeda U. Cardiac overexpression of monocyte chemoattractant protein-1 in transgenic mice prevents cardiac dysfunction and remodeling after myocardial infarction. Circ Res. 2006; 99:891–899. [PubMed: 16990567]

50. Tongers J, Roncalli JG, Losordo DW. Role of endothelial progenitor cells during ischemia-induced vasculogenesis and collateral formation. Microvasc Res. 2010; 79:200–206. [PubMed: 20144623]

51. Tillmanns J, Rota M, Hosoda T, Misao Y, Esposito G, Gonzalez A, Vitale S, Parolin C, Yasuzawa-Amano S, Muraski J, De Angelis A, Lecapitaine N, Siggins RW, Loredo M, Bearzi C, Bolli R, Urbanek K, Leri A, Kajstura J, Anversa P. Formation of large coronary arteries by cardiac progenitor cells. Proc Natl Acad Sci U S A. 2008; 105:1668–1673. [PubMed: 18216245]

52. Bearzi C, Leri A, Lo Monaco F, Rota M, Gonzalez A, Hosoda T, Pepe M, Qanud K, Ojaimi C, Bardelli S, D'Amario D, D'Alessandro DA, Michler RE, Dimmeler S, Zeiher AM, Urbanek K, Hintze TH, Kajstura J, Anversa P. Identification of a coronary vascular progenitor cell in the human heart. Proc Natl Acad Sci U S A. 2009; 106:15885–15890. [PubMed: 19717420]

53. Jujo K, Hamada H, Iwakura A, Thorne T, Sekiguchi H, Clarke T, Ito A, Misener S, Tanaka T, Klyachko E, Kobayashi K, Tongers J, Roncalli J, Tsurumi Y, Hagiwara N, Losordo DW. Cxcr4

blockade augments bone marrow progenitor cell recruitment to the neovasculature and reduces mortality after myocardial infarction. Proc Natl Acad Sci U S A. 2010; 107:11008–11013. [PubMed: 20534467]

54. Beohar N, Rapp J, Pandya S, Losordo DW. Rebuilding the damaged heart: the potential of cytokines and growth factors in the treatment of ischemic heart disease. J Am Coll Cardiol. 2010; 56:1287–1297. [PubMed: 20888519]
55. Rubanyi GM. Mechanistic, technical, and clinical perspectives in therapeutic stimulation of coronary collateral development by angiogenic growth factors. Mol Ther. 2013; 21:725–738. [PubMed: 23403495]
56. Zhang S, Ge J, Zhao L, Qian J, Huang Z, Shen L, Sun A, Wang K, Zou Y. Host vascular niche contributes to myocardial repair induced by intracoronary transplantation of bone marrow CD34+ progenitor cells in infarcted swine heart. Stem Cells. 2007; 25:1195–1203. [PubMed: 17272498]
57. Vandervelde S, van Luyn MJ, Rozenbaum MH, Petersen AH, Tio RA, Harmsen MC. Stem cell-related cardiac gene expression early after murine myocardial infarction. Cardiovasc Res. 2007; 73:783–793. [PubMed: 17208206]
58. Boyle AJ, Yeghiazarians Y, Shih H, Hwang J, Ye J, Sievers R, Zheng D, Palasubramaniam J, Palasubramaniam D, Karschimkus C, Whitbourn R, Jenkins A, Wilson AM. Myocardial production and release of mcp-1 and sdf-1 following myocardial infarction: Differences between mice and man. J Transl Med. 2011; 9:150. [PubMed: 21910857]
59. Italiani P, Boraschi D. From monocytes to M1/M2 macrophages: phenotypical vs. functional differentiation. Front Immunol. 2014; 5:514. [PubMed: 25368618]
60. Martinez FO, Gordon S. The M1 and M2 paradigm of macrophage activation: time for reassessment. F1000Prime Rep. 2014; 6:13. [PubMed: 24669294]
61. Kolattukudy PE, Niu J. Inflammation, endoplasmic reticulum stress, autophagy, and the monocyte chemoattractant protein-1/CCR2 pathway. Circ Res. 2012; 110:174–189. [PubMed: 22223213]
62. Tarzami ST, Calderon TM, Deguzman A, Lopez L, Kitsis RN, Berman JW. MCP-1/CCL2 protects cardiac myocytes from hypoxia-induced apoptosis by a G(alphai)-independent pathway. Biochem Biophys Res Commun. 2005; 335:1008–1016. [PubMed: 16102724]
63. Weir RA, Murphy CA, Petrie CJ, Martin TN, Clements S, Steedman T, Wagner GS, McMurray JJ, Dargie HJ. Monocyte chemoattractant protein-1: A dichotomous role in cardiac remodeling following acute myocardial infarction in man? Cytokine. 2010; 50:158–162. [PubMed: 20299238]
64. Schenk S, Mal N, Finan A, Zhang M, Kiedrowski M, Popovic Z, McCarthy PM, Penn MS. Monocyte chemotactic protein-3 is a myocardial mesenchymal stem cell homing factor. Stem Cells. 2007; 25:245–251. [PubMed: 17053210]
65. Maddaluno M, Di Lauro M, Di Pascale A, Santamaria R, Guglielmotti A, Grassia G, Ialenti A. Monocyte chemotactic protein-3 induces human coronary smooth muscle cell proliferation. Atherosclerosis. 2011; 217:113–119. [PubMed: 21536288]
66. Butoi ED, Gan AM, Manduteanu I, Stan D, Calin M, Pirvulescu M, Koenen RR, Weber C, Simionescu M. Cross talk between smooth muscle cells and monocytes/activated monocytes via CX3CL1/CX3CR1 axis augments expression of pro-atherogenic molecules. Biochem Biophys Acta. 2011; 1813:2026–2035. [PubMed: 21888931]
67. White GE, Greaves DR. Fractalkine: a survivor's guide: chemokines as anti-apoptotic mediators. Arterioscler Thromb Vasc Biol. 2012; 32:589–594. [PubMed: 22247260]
68. Zernecke A, Weber C. Chemokines in the vascular inflammatory response of atherosclerosis. Cardiovasc Res. 2010; 86:192–201. [PubMed: 20007309]
69. Xuan W, Liao Y, Chen B, Huang Q, Xu D, Liu Y, Bin J, Kitakaze M. Detrimental effect of fractalkine on myocardial ischaemia and heart failure. Cardiovasc Res. 2011; 92:385–393. [PubMed: 21840883]
70. Liu H, Jiang D. Fractalkine/CX3CR1 and atherosclerosis. Clin Chim Acta. 2011; 412:1180–1186. [PubMed: 21492740]
71. Tang J, Wang J, Yang J, Kong X, Zheng F, Guo L, Zhang L, Huang Y. Mesenchymal stem cells over-expressing sdf-1 promote angiogenesis and improve heart function in experimental myocardial infarction in rats. Eur J Cardiothorac Surg. 2009; 36:644–650. [PubMed: 19524448]

72. Tang YL, Zhu W, Cheng M, Chen L, Zhang J, Sun T, Kishore R, Phillips MI, Losordo DW, Qin G. Hypoxic preconditioning enhances the benefit of cardiac progenitor cell therapy for treatment of myocardial infarction by inducing CXCR4 expression. Circ Res. 2009; 104:1209–1216. [PubMed: 19407239]

73. Takeda Y, Costa S, Delamarre E, Roncal C, Leite de Oliveira R, Squadrito ML, Finisguerra V, Deschoemaeker S, Bruyère F, Wenes M, Hamm A, Serneels J, Magat J, Bhattacharyya T, Anisimov A, Jordan BF, Alitalo K, Maxwell P, Gallez B, Zhuang ZW, Saito Y, Simons M, De Palma M, Mazzone M. Macrophage skewing by Phd2 haplodeficiency prevents ischaemia by inducing arteriogenesis. Nature. 479(7371):122–126. [PubMed: 21983962]

74. Spring H, Schuler T, Arnold B, Hammerling GJ, Ganss R. Chemokines direct endothelial progenitors into tumor neovessels. Proc Natl Acad Sci U S A. 2005; 102:18111–18116. [PubMed: 16326806]

75. Yamamoto K, Takahashi T, Asahara T, Ohura N, Sokabe T, Kamiya A, Ando J. Proliferation, differentiation, and tube formation by endothelial progenitor cells in response to shear stress. J Appl Physiol. 2003; 95:2081–2088. [PubMed: 12857765]

76. DiPersio JF. Diabetic stem-cell "mobilopathy". N Engl J Med. 2011; 365:2536–2538. [PubMed: 22204729]

77. Sanganalmath SK, Stein AB, Guo Y, Tiwari S, Hunt G, Vincent RJ, Huang Y, Rezazadeh A, Ildstad ST, Dawn B, Bolli R. The beneficial effects of postinfarct cytokine combination therapy are sustained during long-term follow-up. J Mol Cell Cardiol. 2009; 47:528–535. [PubMed: 19616005]

78. Yin L, Ohanyan V, Pung YF, Delucia A, Bailey E, Enrick M, Stevanov K, Kolz CL, Guarini G, Chilian WM. Induction of vascular progenitor cells from endothelial cells stimulates coronary collateral growth. Circ Res. 2012; 110:241–252. [PubMed: 22095729]

79. Przyklenk K, Vivaldi MT, Arnold JM, Schoen FJ, Kloner RA. Capillary anastomoses between the left anterior descending and circumflex circulations in the canine heart: Possible importance during coronary artery occlusion. Microvasc Res. 1986; 31:54–65. [PubMed: 3959915]

80. le Noble F, Fleury V, Pries A, Corvol P, Eichmann A, Reneman RS. Control of arterial branching morphogenesis in embryogenesis: go with the flow. Cardiovasc Res. 2005; 65:619–628. [PubMed: 15664388]

81. Avolio E, Meloni M, Spencer HL, Riu F, Katare R, Mangialardi G, Oikawa A, Rodriguez-Arabaolaza I, Dang Z, Mitchell K, Reni C, Alvino VV, Rowlinson J, Livi U, Cesselli D, Angelini G, Emanueli C, Beltrami AP, Madeddu P. Combined intramyocardial delivery of human pericytes and cardiac stem cells additively improves the healing of mouse infarcted hearts through stimulation of vascular and muscular repair. Circ Res. 2015; 116:e81–e94. [PubMed: 25801898]

82. Tirziu D, Jaba IM, Yu P, Larrivée B, Coon BG, Cristofaro B, Zhuang ZW, Lanahan AA, Schwartz MA, Eichmann A, Simons M. Endothelial nuclear factor-κB-dependent regulation of arteriogenesis and branching. Circulation. 2012; 126:2589–2600. [PubMed: 23091063]

83. Moraes F, Paye J, Mac Gabhann F, Zhuang ZW, Zhang J, Lanahan AA, Simons M. Endothelial cell-dependent regulation of arteriogenesis. Circ Res. 2013; 113:1076–1086. [PubMed: 23897694]

84. Stein O, Dabach Y, Ben-Naim M, Halperin G, Stein Y. Lower macrophage recruitment and atherosclerosis resistance in FVB mice. Atherosclerosis. 2006; 189:336–341. [PubMed: 16494884]

85. Dragneva G, Korpisalo P, Ylä-Herttuala S. Promoting blood vessel growth in ischemic diseases: challenges in translating preclinical potential into clinical success. Dis Model Mech. 2013; 6:312–322. [PubMed: 23471910]

Highlights

- 1st demonstration that *de-novo* neo-collateral formation (NCF) occurs after acute MI
- Neo-collaterals form rapidly in 1–2 days; formation varies with genetic background
- Infarct volume and recovery of pump function correlate with amount of NCF
- Bone-marrow myeloid cells, MCP→CCR2 and fractalkine→CX_3CR1 signaling are required
- NCF may speed immune/progenitor cell delivery to aid regeneration & scar formation

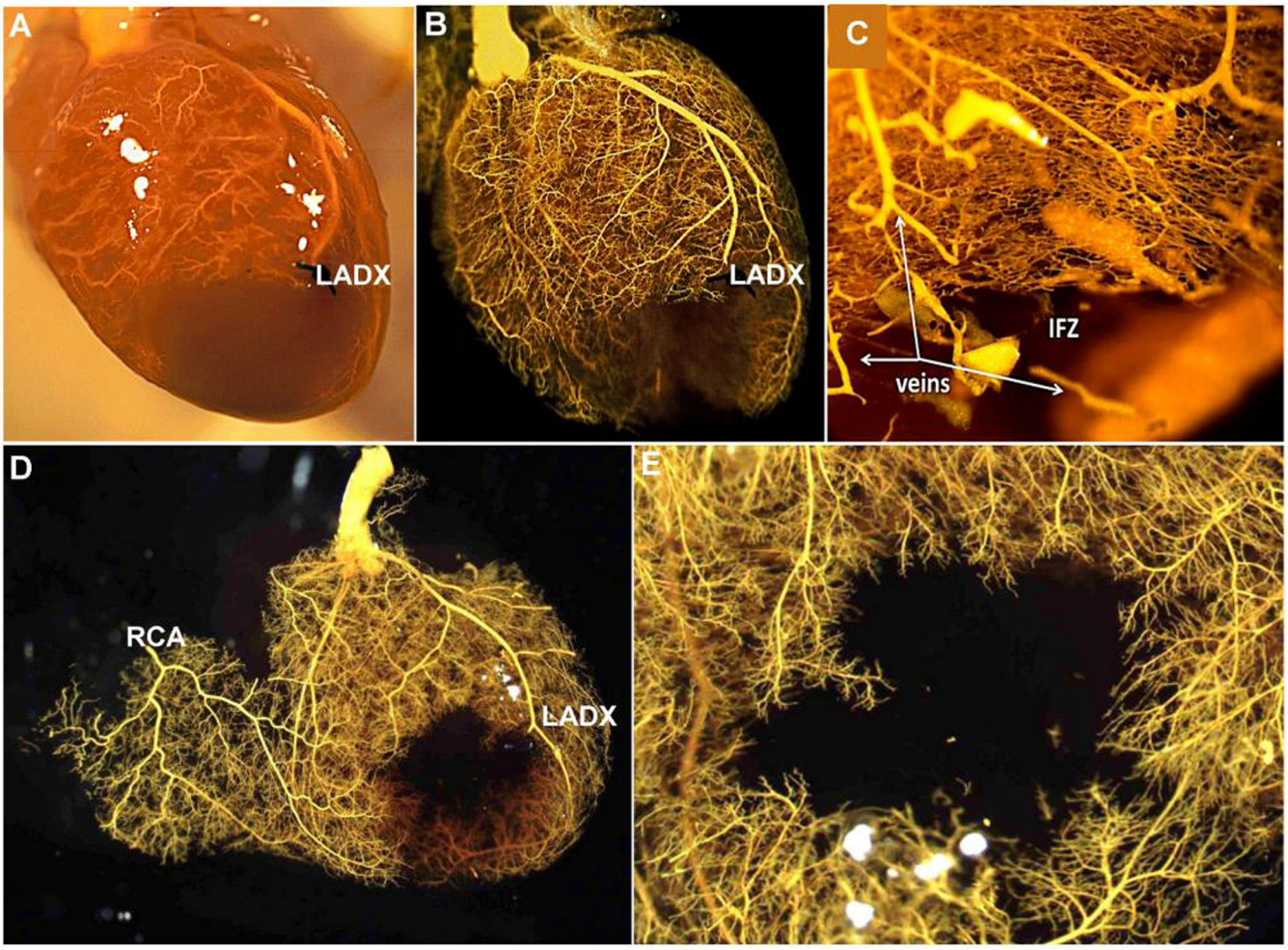

Figure 1. Mice lack native coronary collaterals

A–E, Three months-old C57BL/6 (B6) mice received acute ligation of the distal left anterior descending artery (LADX), followed by coronary infusion at 100 mmHg of papavarine and nitroprusside in PBS for maximal dilation, then 4% paraformaldehyde (PFA); Microfil^{R} was then infused at a viscosity and pressure that fills all pre-capillary vessels. **Panel A** is before and **B–E** are after optical clearing with methyl salicylate. Absence of Microfil^{R} in the LAD artery tree below the ligation (infarct zone, IFZ), including in C where capillaries and some venules were also filled by using a higher pressure, indicates absence of native collaterals is not from failure to fill the smallest-diameter vessels. **D**, RCA, right coronary artery. **E**, Higher magnification of panel D from endocardial side. Data are representative of ≥ 10 B6 adults. The same lack of collaterals was obtained in: adult BALB/c, A/J, C57BLKS (BLKS), SJL, CBA, DBA/2, C3H-He and CD1 strains (≥ 5 of each strain); after transection of the LAD below the ligation to create a minimum-resistance pathway; after endothelial staining using ephrin-B2$^{LacZ/+}$ B6 mice or infusion of the coronary circulation with isolectin-B4-Alex568; and during perfusion with Evans blue-PBS (see Online Figures 1–5) (≥ 3 mice per last 4 procedures).

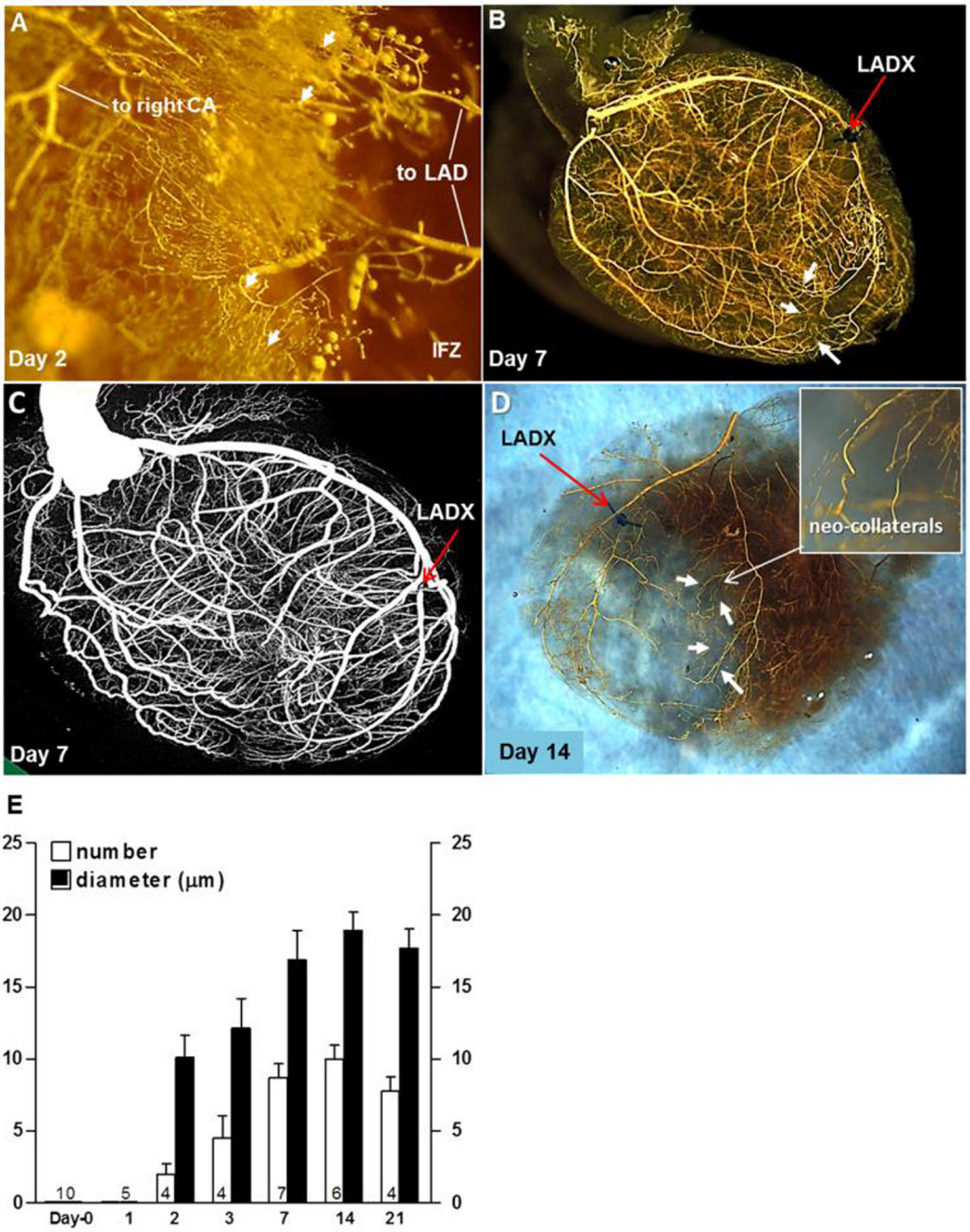

Figure 2. New collaterals rapidly form in mice after ligation of the distal LAD tree (LADX)

The "neo-collaterals " cross-connect the LAD tree to the right coronary (CA) and septal artery trees. Same methods as in Figure 1 were used. **A**, Neo-collaterals (arrows) provide partial back-filling of LAD tree 2 days after LADX. IFZ, infarct zone. **B**, Arrows are several superficial neo-collaterals to right coronary artery tree; neo-collaterals on day-7 provide complete back-filling of LAD tree (See also Online Figures 10,12). **C**, Micro-CT imaging with Scanco40 at maximal resolution shows complete back-filling but is unable to resolve neo-collaterals. **D**, Epicardial neo-collaterals (arrows) after removal of the underlying

myocardium and opposite LV wall to aid imaging. **E**, Time-course for neo-collateral formation after LADX in C57BL/6 mice; number (n) of mice given at base of bars in this and subsequent figures. Maximal number and average diameter of the neo-collaterals are achieved by 7 days.

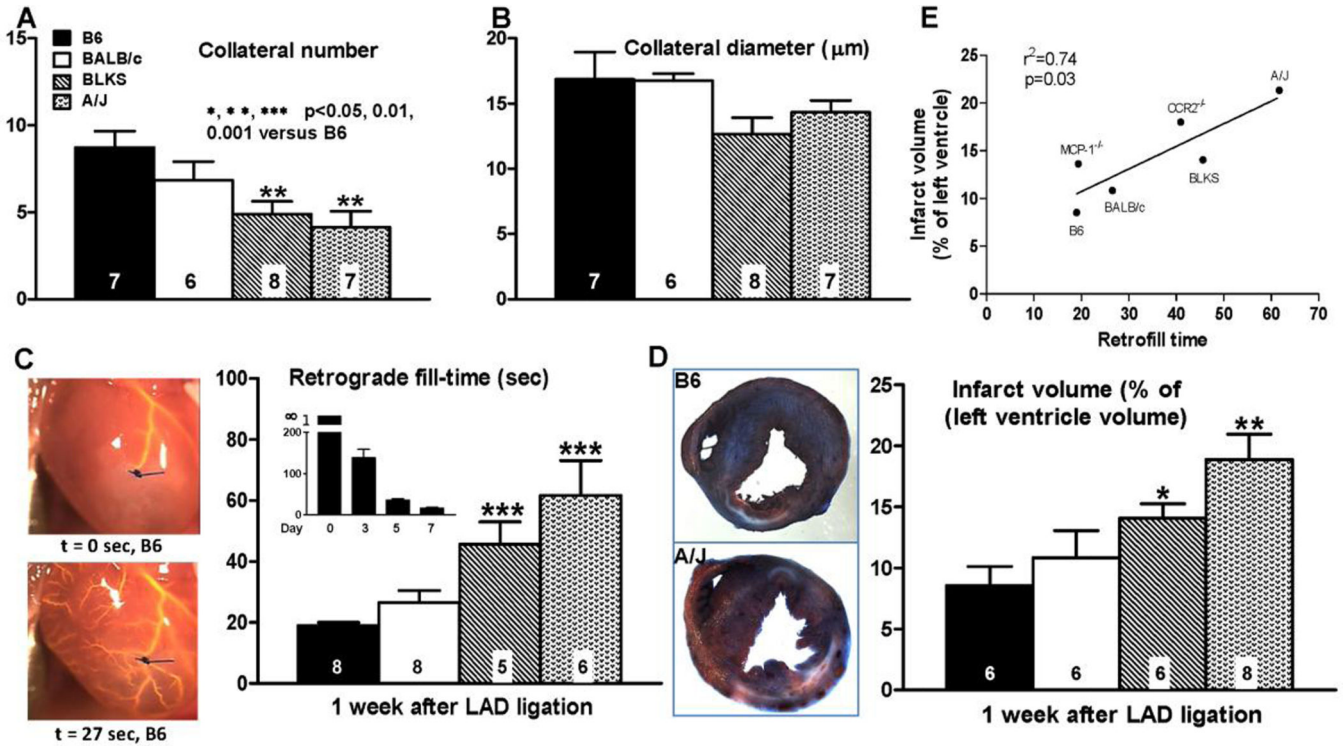

Figure 3. Formation of neo-collaterals after LAD ligation varies with genetic background (A,B) and correlates with relative conductance^{-1} of the newly-formed collateral network (C) and infarct volume (D)

A,B, Number and average diameter determined, as in Figure 2, one week after LADX. **C**, images on left, Time required from start of pump (0 sec) to achieve retrograde filling back to point of ligation of LAD (18 sec, B6 mouse, backfilled branches of LAD evident; See Online figure 10 for video); main bar graph, Microfil^{R} was at same viscosity and pressure for all strains; methods same as in Figure 1 but without optical clearing; insert bar graph, Fill-time on indicated days (n=10,9,4,8 mixed male and female B6 mice); no filling was seen at ≥ 5 min on day-0, consistent with no native collaterals (Figures 1,2), thus time labeled as "infinity" (∞). **D**, Infarct volume. **E**, Infarct volume correlated with retrograde fill-time; MCP-1$^{-/-}$ and CCR2$^{-/-}$ data points are associated with data in Figure 6. Key and statistics in A are for all panels; B6, C57BL/6; BLKS, C57BLKS. Data in panels A-D are from different mice.

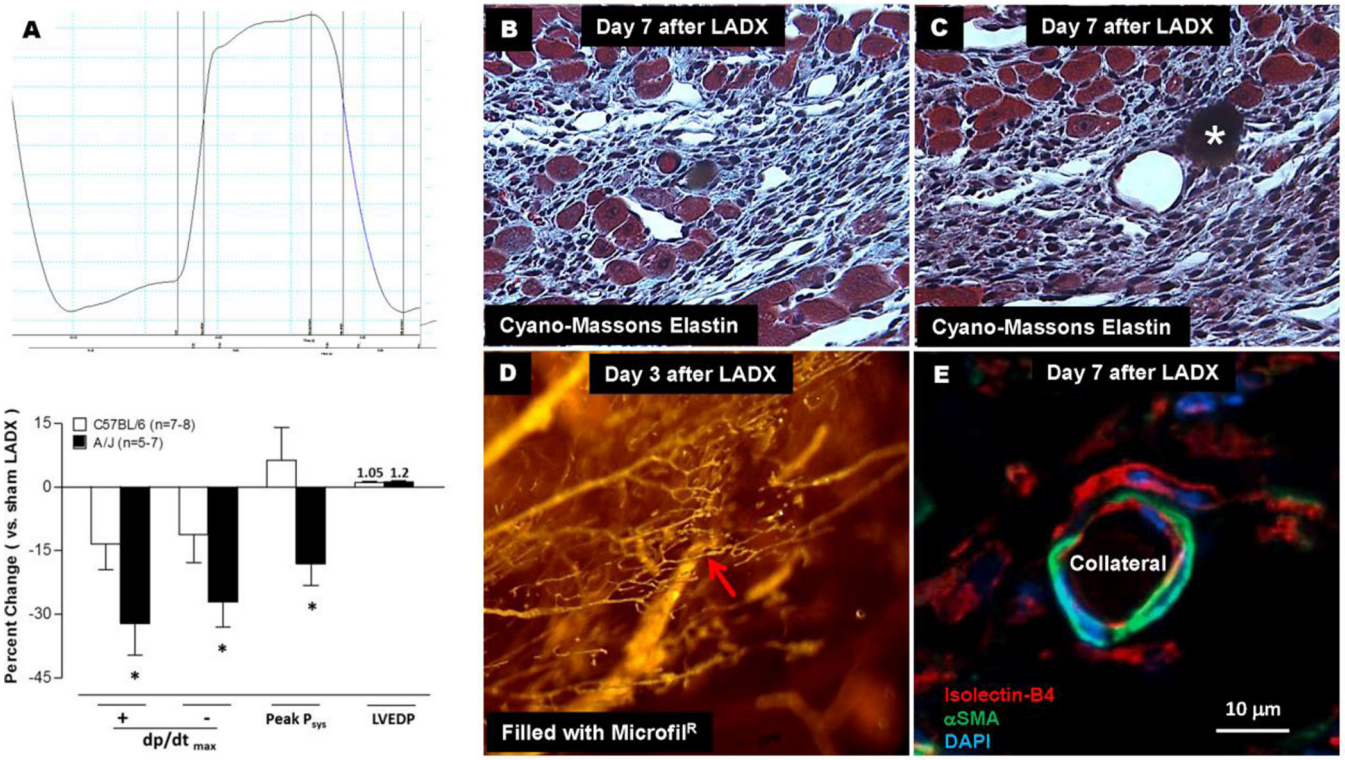

Figure 4. Less neo-collateral formation, less collateral network conductance and larger infarct volume in A/J strain versus B6 strain (see Figure 3) associated with greater deficit in ventricular function (A). Histology of neo-collaterals (B–E)

A, Left ventricular pressure over 1 cardiac cycle. Bottom panel, values determined 7 days after LAD ligation. **B,C**, Neo-collaterals (red arrows, 18 and 45 μm lumen diameter) with Microfil^{R} in lumen (B) or after floating out (C, star). Myocardial cells (large blue-red cells) evident near neo-collaterals and venules. **D**, Endocardial view of piece of ventricular wall bordering the infarct zone with neo-collateral (9 μm) indicated by red arrow. **E**, a-smooth muscle actin^{+} cells surrounding lectin^{+} endothelial cells of a neo-collateral 7 days after ligation; Microfil^{R} can be seen faintly in lumen in this and certain other figures in paper. See Online Figure 12 for methods. Data are representative of ≥ 3 mice at each time-point and each staining.

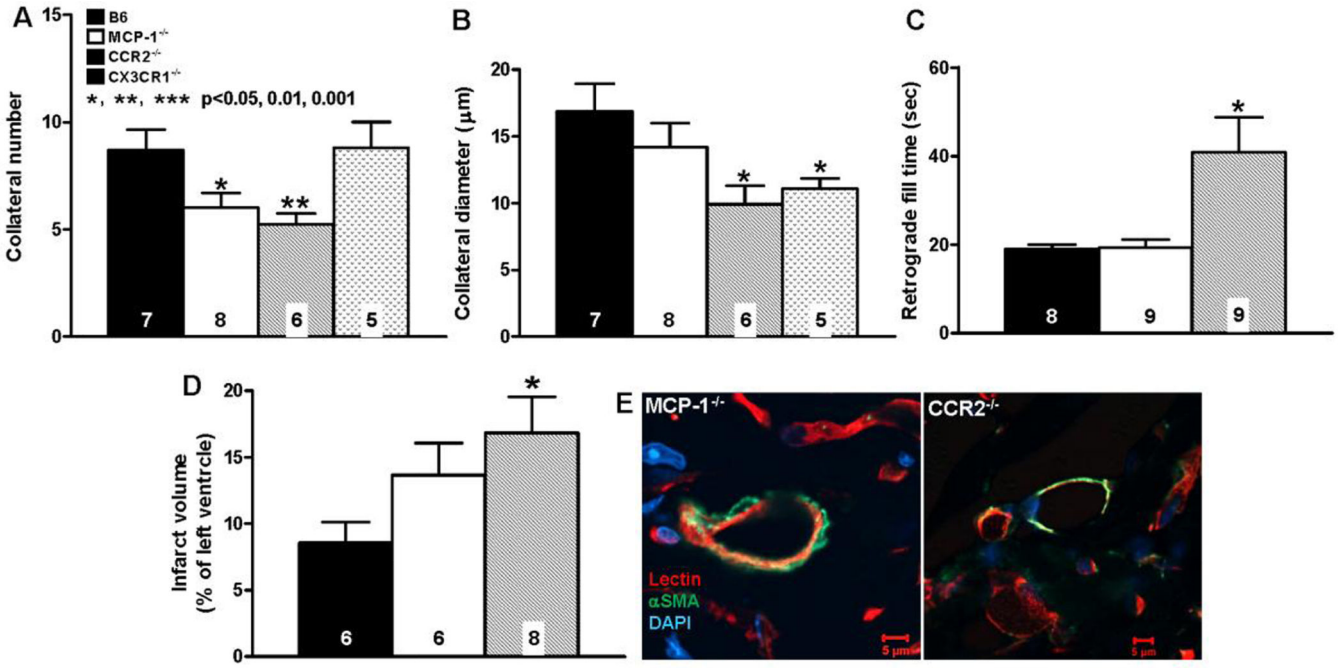

Figure 5. Neo-collateral formation 1 week after LAD ligation is dependent on MCP-1 →CCR2 signaling

A–D, number, diameter, retrograde fill time and infarct volume determined as in Figure 3. $CCR2^{-/-}$ mice have impaired neo-collateral formation. “conductance” and increased infarct volume. $MCP\text{-}1^{-/-}$ show smaller difference from C57BL/6 (B6), possibly owing to other MCP isoforms acting at CCR2. **E**, Neo-collaterals of both $MCP\text{-}1^{-/-}$ and CCR2−/− mice have αSMA^{+} mural cells; magnification bars, 5 um; data are representative of ≥ 3 mice of each. Statistics are versus B6 (background of knockout mice).

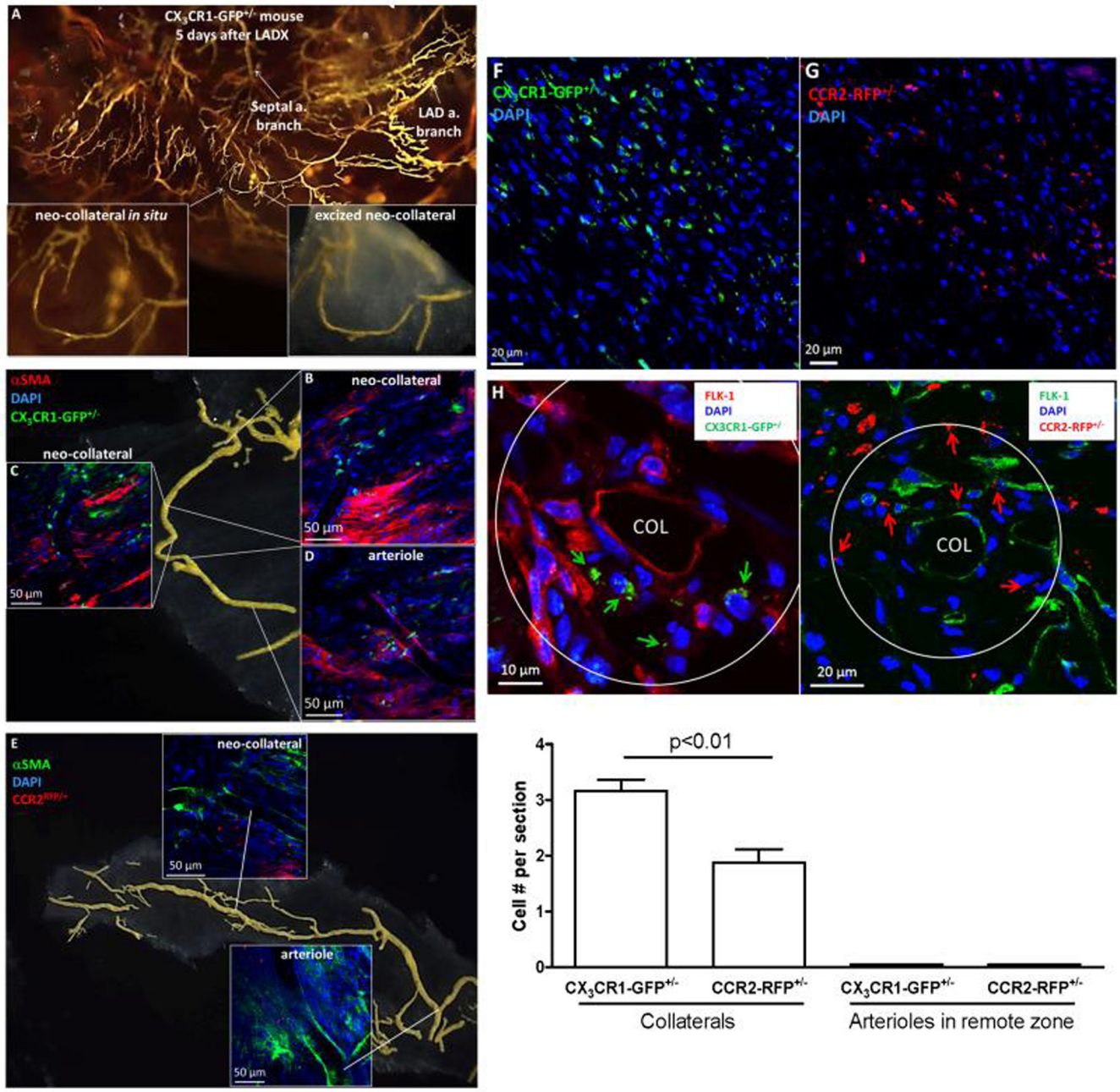

Figure 6. CCR2$^{RFP/+}$ and CX$_3$CR1$^{GFP/+}$ B6 reporter mice show both cell types present throughout border zone and in vicinity of developing neo-collaterals 5 days after LAD ligation

A–E, Whole mount images. αSMA$^+$ mural cells surround neo-collaterals and myofibroblast-like cells present in interstitium. Almost no CCR2$^+$ or CX$_3$CR1$^+$ cells seen in remote zone and none within the vicinity of arterioles or venules (Online Figure 17). **F,G**, 7μm sections from border zone; many fewer CCR2$^+$ or CX$_1$CR3$^+$ cells seen 1 day after LADX (n=5 mice, data not shown). **H**, Neo-collaterals (COL) in border zone. Upper panels: arrows identify both cells types; Flk1$^+$ cells identify endothelial cells of collateral and nearby vessels, and possible monocyte-like EPCs (*). Quantification: cell number counted within area extending

1-collateral diameter outward and averaged for 5 sections separated by 50μm from midpoint of 1 neo-collateral for each mouse; 5 mice 5 days after LADX were studied.

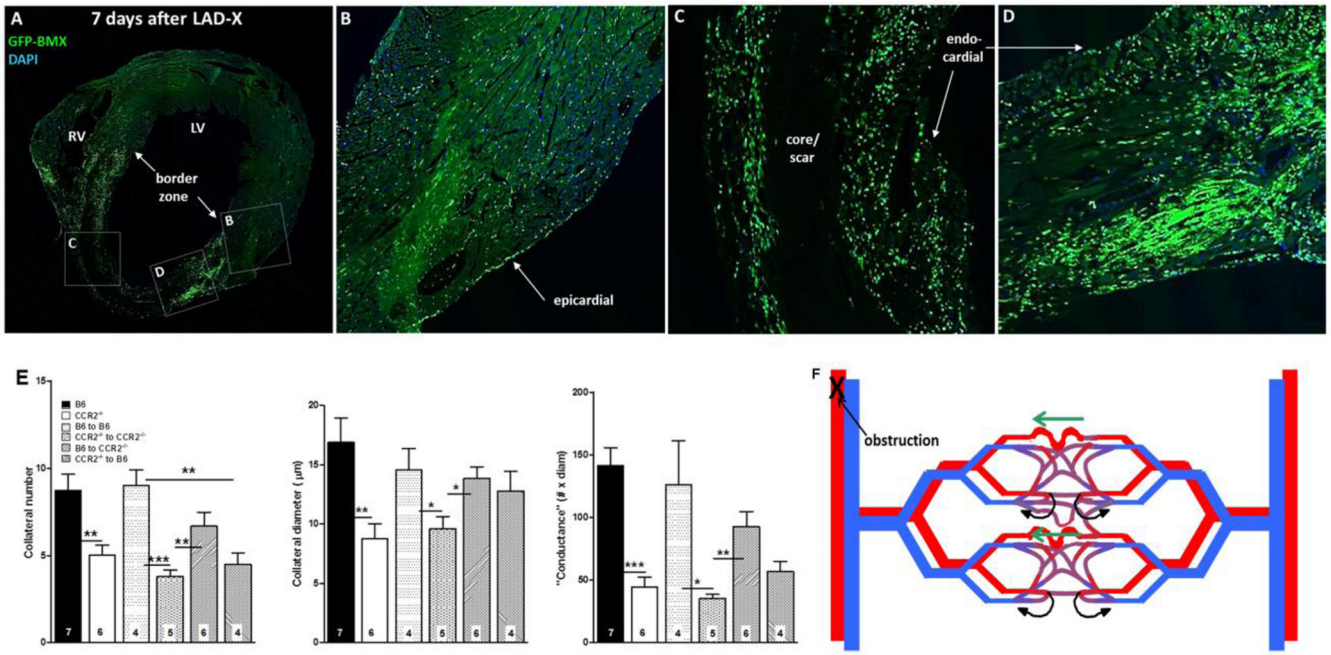

Figure 7.

A–D, Bone-marrow–derived cells home to myocardium. Wildtype B6 mouse 7 weeks after bone-marrow (BM) transplant with B6-GFP-expressing BM cells, and 7 days after LAD ligation. Confocal images (**A**, coronal section of heart at low magnification) show high number of cells in border zone (**A,D**), intermediate number surrounding core/scar region (**A,C**), low number in remote zone (**A,B**) and very low number in core/scar (**A,C**). BM cells also evident in epicardial and endocardial surface layers. **E**, Transplant of wildtype BM cells rescues deficient neo-collateral formation, and transplant of $CCR2^{-/-}$ BM cells inhibits normal neo-collateral formation in wildtype (B6) and $CCR2^{-/-}$ mice 1 week after LAD ligation. Methods are same as in Figure 2. Controls (bars 3 and 4 in each graph) show no effect of the transplant procedure. *, **, *** $p<0.05$, 0.01, 0.001. **Figure 7F. Model of neo-collateral formation**. Blood flow in the capillary plexus in watershed areas between trees normally returns via contiguous venous trees (curved black arrows), consistent with Evans blue perfusion data shown in Online Figures 3–5. Arterial obstruction causes ischemia and increased fluid shear stress, the latter especially in the largest-diameter capillary(s). MCP1, fractalkine and presumably other factors activate CCR2, CX_3CR1 and other proteins, leading to recruitment of immune cells and vascular and/or hematopoietic progenitors from bone marrow and possibly additional sites. The resulting milieu of “remodeling” and growth factors directs pruning of venous connections from the largest capillaries over day 0–1, followed by increase in diameter, length and mural cell recruitment over day 1–7.